

GEORGIA INSTITUTE OF TECHNOLOGY

Competing Excited State Intramolecular Proton Transfer
and Photoinduced Electron Transfer in
2-(2'-Arylsulfonamidophenyl)benzimidazoles

Aneese F. Chaudhry

A Thesis Submitted in Partial Requirements for the
Research Option in School of Chemistry & Biochemistry

Faculty Advisor:
Dr. Christoph Fahrni

Second Reader:
Dr. Robert Dickson

Key Words: excited state intramolecular electron transfer, ESIPT, photoinduced intramolecular electron transfer, PET, fluorescent probes, pH sensor, ratiometric sensing, Hammett free energy relationship

May 5, 2008

Abstract

Cation-induced inhibition of excited-state intramolecular proton transfer (ESIPT) can be effectively utilized to design fluorescent probes for ratiometric Zn(II)-sensing. The 2-(2'-sulfonamidophenyl)benzimidazole family of fluorophores undergoes efficient ESIPT in protic solvents to yield a highly Stokes-shifted emission of the phototautomer. Upon coordination of Zn(II), ESIPT is disrupted and results in a strongly blue-shifted fluorescence emission. Because Zn(II)-binding competes with protonation of the sulfonamide nitrogen, the coordination equilibrium can principally be tuned by adjusting the sulfonamide pK_a . In this study we specifically addressed the question to what extent tuning of the pK_a influences the photophysical properties of this class of fluorophores. For this purpose, a series of compounds with varying substituents attached to the sulfonamide aryl-ring were characterized in terms of their pK_a , their absorption and emission energies, as well as their quantum yields. Although the pK_a varied over almost two orders of magnitude following closely Hammett's free energy relationship, the peak absorption and emission energies remained largely unaltered. Interestingly, the quantum yields of derivatives with strongly electron withdrawing substituents were significantly lower compared to all other fluorophores, suggesting a photoinduced electron transfer process as a possible non-radiative deactivation pathway. Electrochemical analysis revealed indeed an additional reduction wave at a less negative potential for the quenched derivatives. Estimates of the electron transfer driving force based on the Rehm-Weller formalism supported the PET pathway. Furthermore, the quenching mechanism was confirmed through quantum chemical calculations. The findings of this study are expected to aid in the rational design of ESIPT fluorophores for zinc-sensing applications.

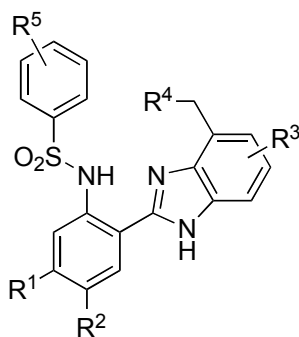
1. Introduction

Zinc is an essential trace element required for the normal growth and viability of organisms and plays a critical role in cellular processes, including reproduction, growth, and regulation as well as various enzymatic activities. Increased levels of zinc in cells have been known to cause cell death,¹ while deficiencies can result in a host of clinical conditions, such as impaired growth,² immune disorders,³ and impaired neuropsychological functions.⁴

Although most intracellular zinc is bound to proteins and the concentration of free zinc is low, these protein-metal complexes undergo fast exchange with the extracellular environment, which indicates the presence of labile pools of zinc. Evidence for these labile pools comes from histochemical autometallographic techniques⁵ that, although informative, are not useful for live cell imaging. A popular alternative utilizes zinc-selective fluorescent probes that passively diffuse into the cell and exhibit an increase in fluorescence intensity upon binding to zinc. Although this method can be used to visualize cellular zinc,^{6,7} the fluorescence emission intensity is dependent not only on metal concentration but also on the ligand concentration, as well as other factors such as variations in incubation time, temperature, membrane permeability, and cell size. As a result, the response from these probes provides only qualitative information regarding the whereabouts of zinc. Quantitative information can be obtained using ratiometric probes, which exhibit a spectral shift upon binding to the metal cation. The ratio of the emission intensities at two excitation or emission wavelengths is independent of the probe concentration, path length, and spectral sensitivity of the instrument and varies only as a function of the cation concentration.⁸

A series of 2-(2'-arylsulfonamidophenyl)benzimidazole derivatives were previously evaluated as potential ratiometric Zn(II)-sensors.⁸⁻¹¹ These compounds undergo excited state intramolecular proton transfer (ESIPT) when the proton covalently attached to the amino group of the amidophenyl moiety migrates in the electronically excited state to a neighboring hydrogen-bonded atom less than 2 angstroms away.⁹ The resulting phototautomer emits light and thermally equilibrates back to the ground state with the proton bound to the original atom.⁹ Upon binding to zinc, however, the proton is replaced, and ESIPT is inhibited, which results in a blue shifted emission. Optimization of the probe for biological applications requires tuning of the pK_a in order to maintain the species protonated at cellular pH levels.

The photophysical properties of the benzimidazole derivatives can be tuned by varying substituents for R^1 , R^2 , and R^3 , while variation at R^4 allows tuning of the zinc binding affinity. Theoretically, pK_a tuning is possible with variation of the R^5 substituent on the arylsulfonamide moiety, but the impact of this substitution on the photophysics of the system is unknown. How will substitution influence proton transfer kinetics, absorption and emission energies, and quantum yield? The ability to tune the pK_a of this system without negatively influencing its previously optimized photophysics will place the final piece in the puzzle and allow the commencement of intracellular zinc studies.



2. Experimental Section

Synthesis: All compounds were prepared in a one-step synthesis from commercially available reagents. The crude products were recrystallized using a diethyl ether/ethyl acetate/hexane solvent mixture. The chemical structures of the synthesized compounds were confirmed by ^1H NMR, mass spectrometry (MS) and high-resolution mass spectrometry.

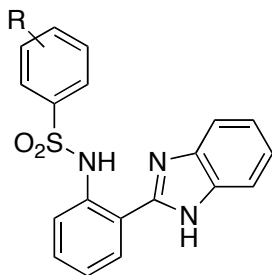
Absorption and Fluorescence Spectroscopy: UV-vis absorption spectra were recorded at 25 °C using a Varian Cary Bio50 UV-vis spectrometer. For all measurements the path length was 1 cm with a cell volume of 3.0 mL. The fluorescence spectra have been corrected for the spectral response of the detection system (emission correction file provided by instrument manufacturer) and for the spectral irradiance of the excitation channel (via calibrated photodiode). Quantum yields were determined using quinine sulfate dihydrate in 1.0 N H_2SO_4 as the fluorescence standard ($\Phi_f = 0.54 \pm 0.05$).¹²

Cyclic Voltammetry: The cyclic voltammograms were acquired in acetonitrile containing 0.1M Bu_4NPF_6 as electrolyte using a CH-Instruments potentiostat (Model 600A). The samples were measured under inert gas at a concentration of 3 mM in a single compartment cell with a glassy carbon working electrode, a Pt counter electrode, and a Ag/AgNO_3 (10 mM in CH_3CN) non-aqueous reference electrode. The half-wave potentials were referenced to ferrocene as the internal standard. All measurements were performed with a scan rate of 100 mVs^{-1} .

3. Results and Discussion

3.1 Fluorophore Design and Synthesis. In order to systematically investigate the influence of the sulfonamide nitrogen pK_a on the photophysical properties, we synthesized a series of compounds with varying substituents attached to the sulfonamide aryl ring (Chart 1). All derivatives were accessible in a single synthetic step starting from commercially available 2-aminophenylbenzimidazole and the corresponding arylsulfonyl chloride. The coupling reactions were carried out under mild conditions at ambient temperature and provided the desired products **1a-1l** in analytical purity after a single recrystallization step.

Chart 1



Compound	R
1a	<i>p</i> -NH ₂
1b	<i>p</i> -OMe
1c	<i>p</i> -Me
1d	H
1e	<i>p</i> -F
1f	<i>m</i> -OMe
1g	<i>p</i> -Cl
1h	<i>m</i> -F
1i	<i>m</i> -Cl
1j	<i>m</i> -CN
1k	<i>p</i> -SO ₂ Me
1l	<i>p</i> -CN

3.2 Protonation Equilibria. Due to insufficient solubility of compounds **1a-l** in aqueous solution, the pK_a titrations were performed in a mixture of methanol and water (50/50 w/w) with 0.1 M KCl as the ionic background. The emf response of the electrode in this solvent mixture was calibrated based on accurately known concentrations of acid

using Gran's method. The pH readings correspond therefore to actual proton concentrations (referred to as p_cH) and not their activity. As illustrated with the titration curve of the methoxy-substituted derivative **1b** (Figure 1), deprotonation of the sulfonamide occurs in the basic region at $p_cH = 8.66 \pm 0.02$. To determine the pK_a for protonation of the benzimidazole ring nitrogen, the titration solution was acidified with 1.08 molar equiv of HCl. Non-linear least-square fitting revealed a pK_a around 3.69 ± 0.04 , a value that is considerably lower compared to the structurally analogous 2-(2'-hydroxyphenyl)-substituted benzimidazole (pK_a 5.90).¹³ For the aminophenyl compound protonation of the imidazole nitrogen requires an out of plane rotation of the benzimidazole due to steric interaction with the neighboring protonated amine, which results in a loss of conjugation and overall destabilization of the molecule (Scheme 1, A). In the hydroxyphenyl compound, on the other hand, protonation results in added stability from the intramolecular hydrogen bonding of the protonated imidazole with the neighboring oxygen (Scheme 1, B). This stabilization of the conjugate acid is reflected in the higher pK_a value of the hydroxyphenyl compound.

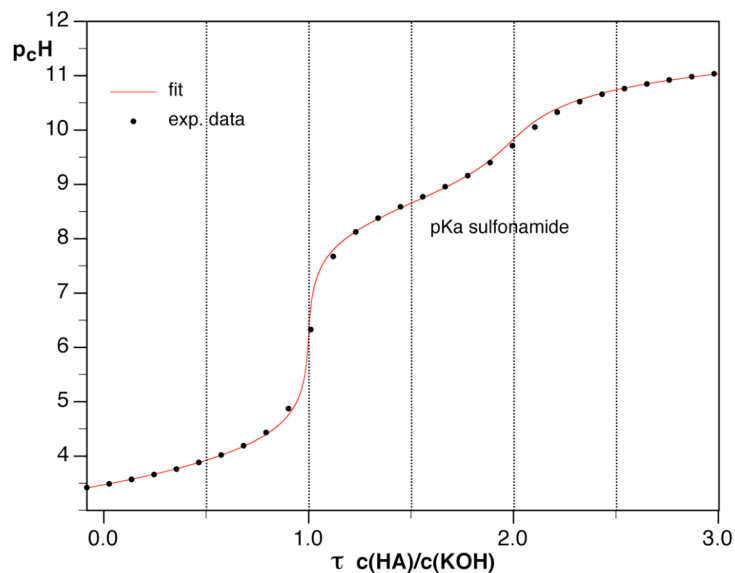
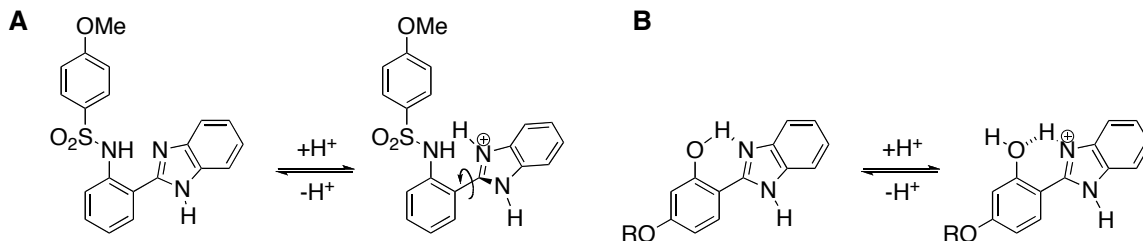


Figure 1. Experimental data and curve fit for the titration of the *p*-OMe substituted arylsulfonamide derivative **1b** with KOH in MeOH-H₂O (50/50 w/w). The solution was acidified with 1.08 molar equiv of HCl to evaluate also the pK_a for protonation of the imidazole nitrogen.

Scheme 1



The experimental pK_a values for the derivatives as well as their respective Hammett σ parameters as compiled by Exner are listed in Table 1. The Hammett parameters, defined by the Hammett free energy relationship, are a measure of the electron-withdrawing or electron-donating ability of a substituent, with positive values corresponding to increasing withdrawing ability and negative values corresponding to increasing donating

ability.¹⁴ The Hammett free energy relationship provides a means of quantifying polarity or effective charge through correlation with dissociation equilibria.

Table 1. Thermodynamic Data of Sulfonamide Derivatives **1a-1l** in Methanol-Water (50/50 w/w) at 298 K.

	R	Hammett parameter σ	pK_a
1a	<i>p</i> -NH ₂	-0.30	9.23
1b	<i>p</i> -OMe	-0.12	8.76
1c	<i>p</i> -Me	-0.14	8.64
1d	H	0.00	8.40
1e	<i>p</i> -F	0.15	8.26
1f	<i>m</i> -OMe	0.10	8.43
1g	<i>p</i> -Cl	0.24	8.07
1h	<i>m</i> -F	0.34	7.98
1i	<i>m</i> -Cl	0.37	7.94
1j	<i>m</i> -CN	0.62	7.56
1k	<i>p</i> -SO ₂ Me	0.73	n.d.
1l	<i>p</i> -CN	0.71	7.43

n.d. not determined

A plot of the experimental sulfonamide pK_a values against the Hammett σ parameters provided a good linear correlation with $r = 0.98$ (Figure 2), which indicates that the variation in pK_a values across substituents is largely governed by inductive and resonance effects, with no significant contribution from sterics.

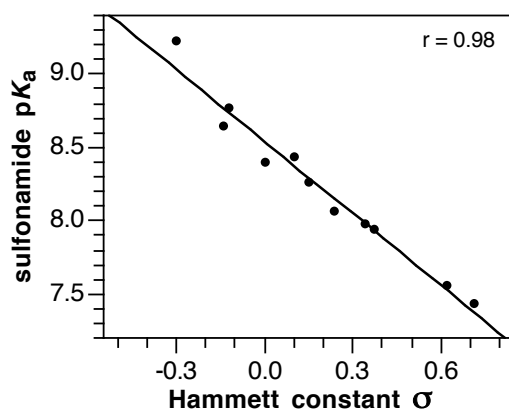


Figure 2. Correlation of the experimental pK_a values measured in water and methanol (50/50 w/w) with Hammett σ parameters.

3.3 Photophysical Properties. A compilation of the photophysical properties for compounds **1a-l** is given in Table 2. All data were measured at 298K under neutral (methanol) and basic (0.1M methanolic sodium methoxide) conditions with good solubility. Within the applied concentration range, normalized absorption spectra were superimposable and scaled linearly, indicating no detectable aggregation. Under neutral conditions, the derivatives display little shift in spectra, for both absorption and emission (Figure 3). There is no effect of substitution on the photophysics of the molecules with regard to spectral shift under neutral conditions. Additionally, under neutral conditions high quantum yields are obtained for many of the compounds, excluding *p*-NH₂, *m*-CN, *p*-SO₂Me, and *p*-CN, which exhibit quenching. Under basic conditions, the quantum yields for the series are largely quenched with the exception of *p*-NH₂ and *p*-OMe, which maintain significant fluorescence with quantum yields of 0.31 and 0.34, respectively.

Table 2. Photophysical Data of Derivatives **1a-1l** in Methanol at 298K.

R	Neutral conditions				Basic conditions			
	Abs λ_{\max} [nm]	Em λ_{\max}^a [nm]	Stokes shift [cm ⁻¹]	Φ_f^b	Abs λ_{\max} [nm]	Em λ_{\max}^c [nm]	Stokes shift [cm ⁻¹]	Φ_f^b
1a <i>p</i> -NH ₂	314	480	11014	0.07	340	424	5827	0.31
1b <i>p</i> -OMe	313	470	10672	0.57	339	418	5575	0.34
1c <i>p</i> -Me	313	467	10536	n.d.	337	417	5693	n.d.
1d H	313	467	10536	n.d.	337	414	5343	n.d.
1e <i>p</i> -F	312	465	10546	0.54	336	411	5431	0.02
1f <i>m</i> -OMe	312	465	10546	0.51	337	413	5461	0.00
1g <i>p</i> -Cl	312	464	10500	0.46	336	407	5009	0.00
1h <i>m</i> -F	313	463	10351	0.42	336	408	5252	0.00
1i <i>m</i> -Cl	312	463	10453	0.40	336	409	5312	0.00
1j <i>m</i> -CN	312	462	10406	0.02	338	405	4894	0.00
1k <i>p</i> -SO ₂ Me	313	456	10019	0.00	333	417	6049	0.00
1l <i>p</i> -CN	313	462	10304	0.00	335	416	5812	0.00

^a excitation wavelength 311-314 nm. ^b fluorescence quantum yield; quinine sulfate as reference. ^c excitation wavelength 330 nm.

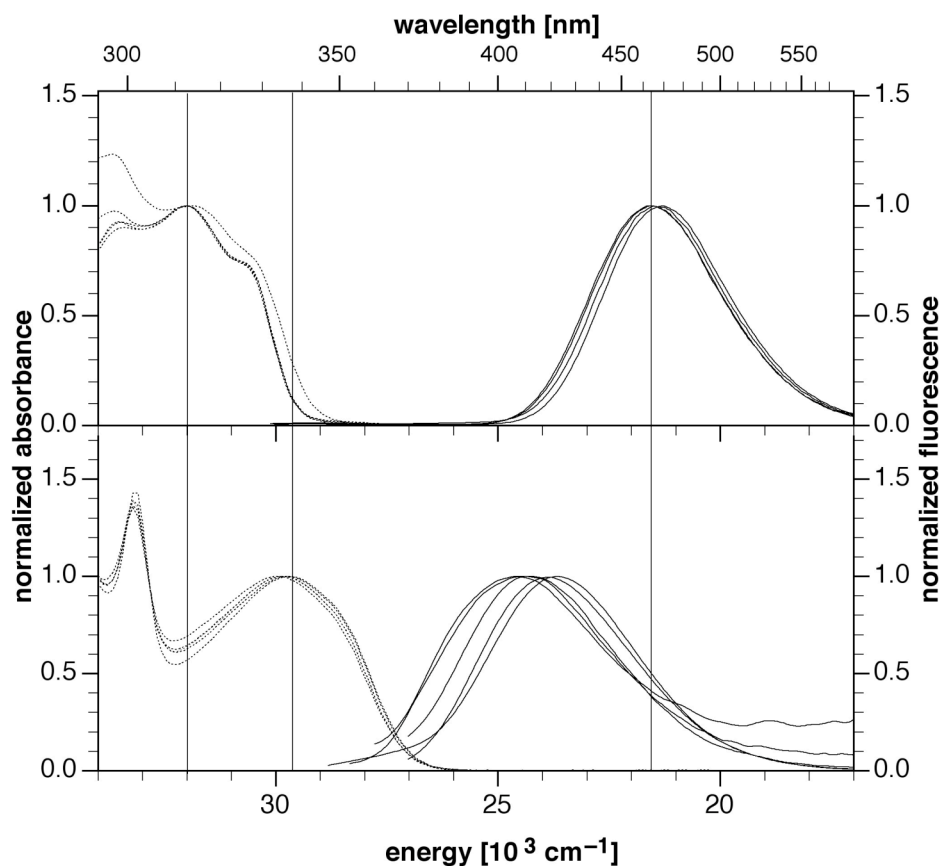


Figure 3. Comparison of the normalized absorption and emission spectra of compounds **1a-l** under neutral (top) and basic (bottom) conditions. Absorption spectra are reproduced with dotted lines and emission spectra with solid traces.

The efficiency of ESIPT might be governed by the excited state pK_a of the sulfonamide proton donor. To investigate whether differences in quantum yield might be due to different excited state acidities, we used Foerster's method to estimate the pK_a^* :

$$pK_a^* = pK_a + 2.1 \times 10^{-3} (\bar{\nu}_{A^-} - \bar{\nu}_{HA}) \quad (1)$$

The wavenumbers $\bar{\nu}_{HA}$ and $\bar{\nu}_{A^-}$ correspond to the 0–0 transitions (ΔE_{00}) of the compounds under neutral (HA) and basic (A-) conditions. The excited state energy of HA cannot be determined with the conventional approach, where ΔE_{00} is calculated as the

average of ν_{abs} and ν_{em} . Upon excitation, the 2-(2'-aminophenyl)benzimidazole molecules undergo ESIPt resulting in a tautomer of a structurally different species, the phototautomer. Therefore the strongly Stokes-shifted tautomer emission cannot be used for the determination of the ΔE_{00} of HA.

In order to determine ΔE_{00} values for HA, the respective absorption spectra were fit using multiple Gaussians, as appropriate, representing the vibronic envelope of a spectrum (Figure 4). A tangent line to the rightmost inflection point of the lowest energy Gaussian was derived and its abscissa determined. The midpoint between the intercept of the tangent line and the peak of the lowest energy vibrational band is used to represent ΔE_{00} under neutral conditions (ΔE_{00} [HA]). The ΔE_{00} for the compounds under basic conditions was simply the midpoint between the absorption and emission maximum (ΔE_{00} [A⁻]). Data for the Foerster cycle is compiled in Table 3 and Figure 5 demonstrates that the observed changes in excited state pK_a^* fall within the range of experimental error.

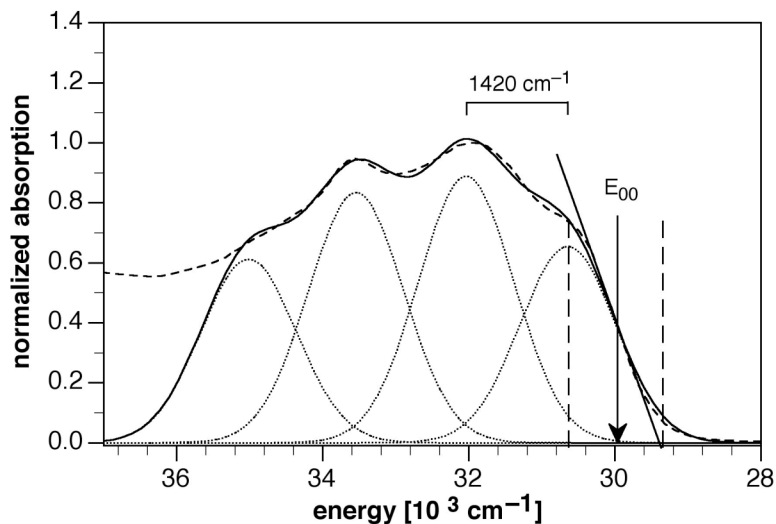
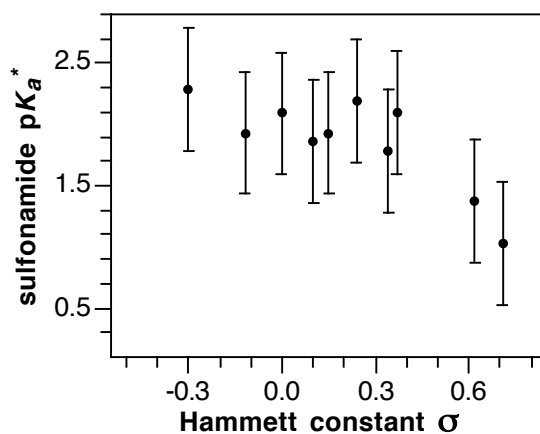


Figure 4. Normalized absorption spectra under neutral conditions (solid line) with corresponding calculated fit (dashed line) and underlying vibrational bands (dotted line); ΔE_{00} is the midpoint between the peak maximum of the lowest energy Gaussian and the x-intercept of the tangent line to its point of inflection.

Table 3. Excited State Energies and pK_a* Estimated based on Förster Cycle

	R	m ^a	ΔE ₀₀ HA [cm ⁻¹]	ΔE ₀₀ A ⁻ [cm ⁻¹]	pK _a *
1a	<i>p</i> -NH ₂	30443	29796	26498	2.29
1b	<i>p</i> -OMe	30526	29963	26711	1.93
1c	<i>p</i> -Me	n.d.	n.d.	26827	n.d.
1d	H	30549	30007	27002	2.09
1e	<i>p</i> -F	30595	30059	27046	1.93
1f	<i>m</i> -OMe	30627	30068	26943	1.86
1g	<i>p</i> -Cl	30593	30053	27257	2.19
1h	<i>m</i> -F	30613	30086	27136	1.78
1i	<i>m</i> -Cl	30618	30082	27302	2.10
1j	<i>m</i> -CN	30610	30080	27139	1.38
1k	<i>p</i> -SO ₂ Me	30529	29962	27005	n.d.
1l	<i>p</i> -CN	30571	29989	26945	1.03

^a m: peak max of the lowest energy vibrational band from the Gaussian fit. ^b zero-zero transition energy, for determination see Figure 5, corresponding text. ^c zero-zero transition energy based on $\Delta E_{00} = (E_{\text{abs}}(\text{max}) + E_{\text{em}}(\text{max}))/2$. ^d excited state protonation equilibrium constant estimated based on $\text{p}K_{\text{a}}^* = \text{p}K_{\text{a}} + 2.1 \times 10^{-3} (\Delta E_{00} [\text{A}^-] - \Delta E_{00} [\text{HA}])$.

**Figure 5.** Correlation of the calculated excited state pK_a* values with Hammett σ parameters, with values falling within the range of experimental error.

A plot of the quantum yields under neutral conditions versus the Hammett σ parameters of the respective derivatives provides a good linear correlation with $r = 0.98$ for the intermediate range of quantum yields (Figure 6). Interestingly, all outliers contain either a strongly electron-donating or strongly withdrawing substituent. It is conceivable

that the sulfonamide moiety acts as an electron accepting group and quenches the fluorescence through photoinduced intramolecular electron transfer (PET).

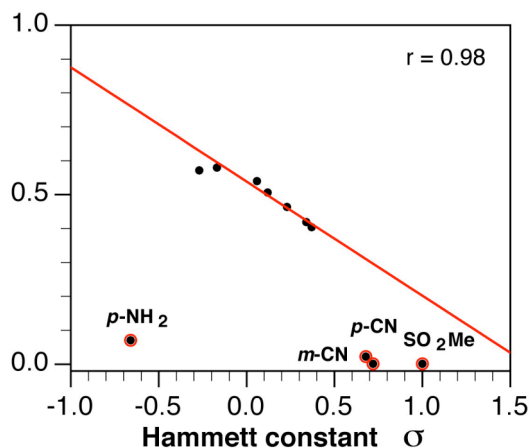
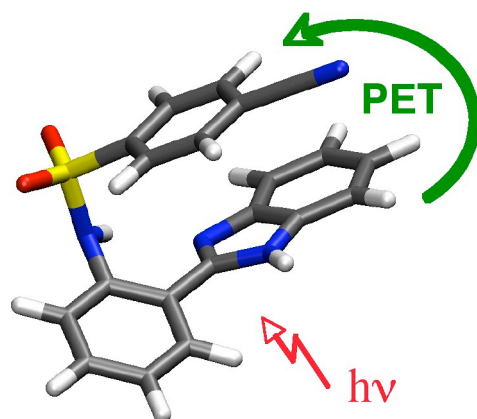


Figure 6. Correlation of quantum yields under neutral conditions in methanol with Hammett σ parameters.

3.4 Evaluation of Electron Transfer Pathway. To test the above hypothesis, we further evaluated the compounds for possible PET pathways upon excitation from the benzimidazole donor to the arylsulfonamide acceptor as seen below. Charge recombination is typically a nonradiative process that would result in quenching of the emission, which would be consistent with the acquired data.

Scheme 2



The rate of electron transfer depends on the free energy change, which if large enough could effectively compete with the rate of ESIPT. According to the Rehm-Weller equation (2), the free energy of electron transfer depends on the donor oxidation potential, acceptor reduction potential, and excited state equilibrium energy.

$$\Delta G_{\text{ET}} = E_{1/2}(\text{D}^+/\text{D}) - E_{1/2}(\text{A}/\text{A}^{\pm}) - \Delta E_{00} \quad (2)$$

The half wave donor and acceptor reduction potentials of the compounds were measured by employing cyclic voltammetry in 0.1M tetrabutylammonium hexafluorophosphate/acetonitrile with ferrocenium internal standard, using millimolar concentrations of the compounds. The free energy of electron transfer was calculated from the Rehm-Weller formalism first using estimated E_{00} values based on the red-edge of the absorption spectra (Table 4). In this case, the ET reaction is predicted to be favorable for all derivatives; however, the measured quantum yields indicate ET quenching only for derivatives **1j-1l**. This inconsistency suggests that ET does not occur from the Franck-Condon state upon excitation of the normal tautomer. If the ET driving force is estimated based on the E_{00} values of the tautomeric species, strong quenching is indeed predicted for derivatives **1i-1l** (Table 4), while the ET reaction should be unfavorable for **1a-1h**. Based on these estimates, the ET rate is slower than the proton transfer process such that quenching can only occur after formation of the phototautomer. Consistent with this conclusion, all of the quenched derivatives (*m*-CN, *p*-SO₂Me, *p*-CN) display an additional nonreversible reduction band at a less negative potential (-2.1 V), indicative of reduction of the sulfonamide unit (Figure 7).

Table 4. Reduction potentials and electron transfer parameters of compounds in acetonitrile at 298K.

	R	$E_{1/2}(D/D^+)$	$E_{1/2}(A/A^-)$	E_{00} [eV] ^a	ΔG_{et} [eV] ^b	ΔG_{et} [eV] ^c
1a	<i>p</i> -NH ₂	0.778	-2.539	2.90	-0.43	0.37
1b	<i>p</i> -OMe	0.857	-2.411	2.95	-0.50	0.27
1c	<i>p</i> -Me	n.d.	n.d.	2.98	n.d.	n.d.
1d	H	n.d.	n.d.	3.02	n.d.	n.d.
1e	<i>p</i> -F	0.854	-2.282	2.98	-0.64	0.10
1f	<i>m</i> -OMe	0.842	-2.302	2.97	-0.63	0.12
1g	<i>p</i> -Cl	0.967	-2.299	2.98	-0.51	0.23
1h	<i>m</i> -F	0.856	-2.299	2.99	-0.63	0.11
1i	<i>m</i> -Cl	0.859	-2.145	2.99	-0.78	-0.04
1j	<i>m</i> -CN	0.899	-2.126	3.00	-0.75	-0.02
1k	<i>p</i> -SO ₂ Me	0.912	-2.011	3.06	-0.84	-0.18
1l	<i>p</i> -CN	0.862	-1.965	3.03	-0.94	-0.25

^aestimated based on emission spectra from Gaussian fit. ^bbased on E_{00} values from absorption spectra. ^cbased on E_{00} values from emission of tautomer species.

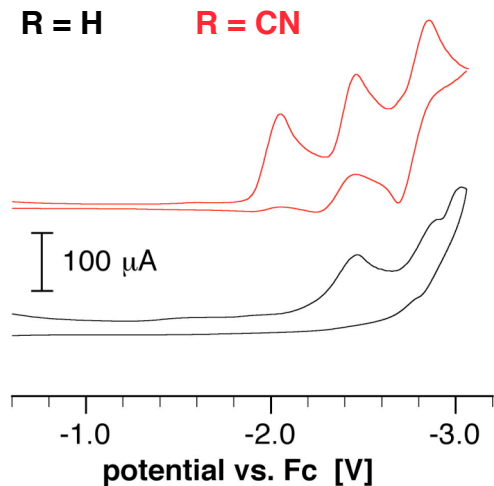


Figure 7. Cyclic voltammograms of the unsubstituted parent compound (R=H) and the *p*-cyano substituted compound in acetonitrile/0.1 M Bu₄NPF₆ versus ferrocenium (Fc⁺⁰).

3.5 Quantum Chemical Calculations. Quantum chemical calculations of the lowest four excited states of the unsubstituted and cyano substituted compounds were also performed, with blue regions indicating the detachment densities and red regions indicating attachment densities with electron flow from the blue to the red region (Figure 8). Analysis of the unsubstituted compound reveals that the S1 excited state corresponds to the lowest emissive state with S4 resembling a high-energy electron transfer state due to the distribution of attachment/detachment densities. Analysis of the cyano substituted derivative reveals that electron transfer states occur at lower energies (S1 and S2) with S3 corresponding to the local emissive state of the unsubstituted compound, which indicates that for the cyano-substituted derivative, excitation to the local excited state is followed by nonradiative emission from the electron transfer state, resulting in quenching of the emission.

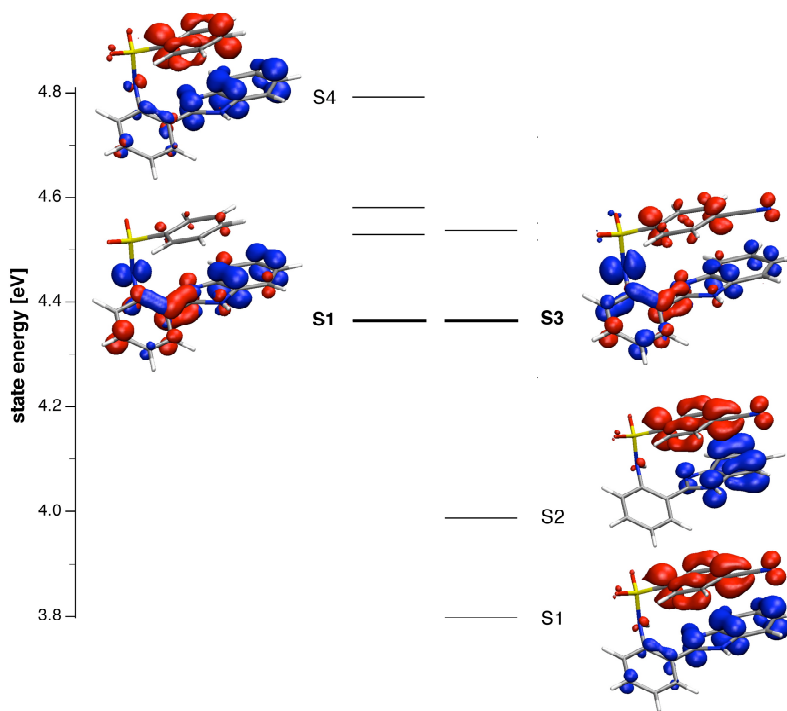


Figure 8. TD-DFT quantum chemical calculations of the unsubstituted (*right*) and cyano substituted (*left*) derivatives (TDDFT (B3LYP/6-31G**//HF/3-21+G**)).

Conclusion

In summary, substitution on the arylsulfonamide moiety exerts little influence on the photophysics of the derivatives, but changes the pK_a , allowing for pK_a tuning without changing the photophysics. Electron-withdrawing substituents on the arylsulfonamide ring introduce a PET pathway that leads to effective quenching. Estimates for the driving force of the ET quenching reaction indicate that formation of the ESIPT species precedes electron transfer quenching. This study lays out a framework for rationally tuning the thermodynamic properties of this class of fluorophores and may aid in the development of metal-selective fluorescent probes based on cation-induced inhibition of excited state intramolecular proton transfer.

Acknowledgments

Financial support by the National Institutes of Health is gratefully acknowledged (DK68096).

References

- (1) Cho, I. H.; Im, J. Y.; Kim, D.; Kim, K. S.; Lee, J. K.; Han, P. L. *Journal of Neuroscience Research* **2003**, *74*, 736.
- (2) Rossi, L.; Migliaccio, S.; Corsi, A.; Marzia, M.; Bianco, P.; Teti, A.; Gambelli, L.; Cianfarani, S.; Paoletti, F.; Branca, F. *Journal of Nutrition* **2001**, *131*, 1142.
- (3) Failla, M. L. *Journal of Nutrition* **2003**, *133*, 1443S.
- (4) Maylor, E. A.; Simpson, E. E. A.; Secker, D. L.; Meunier, N.; Andriollo-Sanchez, M.; Polito, A.; Stewart-Knox, B.; McConville, C.; O'Connor, J. M.; Coudray, C. *British Journal of Nutrition* **2006**, *96*, 752.
- (5) Cole, T. B.; Wenzel, H. J.; Kafer, K. E.; Schwartzkroin, P. A.; Palmiter, R. D. *Proceedings of the National Academy of Sciences of the United States of America* **1999**, *96*, 1716.
- (6) Love, R.; Salazar, G.; Faundez, V. *Brain Research* **2005**, *1061*, 1.
- (7) Chang, C. J.; Nolan, E. M.; Jaworski, J.; Okamoto, K. I.; Hayashi, Y.; Sheng, M.; Lippard, S. J. *Inorganic Chemistry* **2004**, *43*, 6774.

- (8) Henary, M. M.; Wu, Y.; Fahrni, C. J. *Chemistry - A European Journal* **2004**, *10*, 3015.
- (9) Fahrni, C. J.; Henary, M. M.; VanDerveer, D. G. *J. Phys. Chem. A* **2002**, *106*, 7655.
- (10) Henary, M. M.; Wu, Y. G.; Cody, J.; Sumalekshmy, S.; Li, J.; Mandal, S.; Fahrni, C. J. *J. Org. Chem.* **2007**, *72*, 4784.
- (11) Wu, Y.; Lawson, P. V.; Henary, M. M.; Schmidt, K.; Bredas, J. L.; Fahrni, C. J. *J. Phys. Chem. A* **2007**, *111*, 4584.
- (12) Demas, J. N.; Crosby, G. A. *Journal of Physical Chemistry* **1971**, *75*, 991.
- (13) Henary, M. M.; Fahrni, C. J. *J. Phys. Chem. A* **2002**, *106*, 5210.
- (14) Hammett, L. P. *Journal of the American Chemical Society* **1937**, *59*, 96.